WORLD JOURNAL OF PHARMACEUTICAL RESEARCH
SJIF Impact Factor 5.045
Volume 3, Issue 4, 1748-1774. Research Article ISSN 2277 – 7105

MICA NANOPARTICLES CAN BE AN ANTIODOTE FOR MALE GERM LINE: AN ULTRASTRUCTURAL EVALUATION IN WISTAR RATS

***Babita Bhatia[1], Purushottam G Kale[2], Pramod Meshram[3]**

[1]Department of Biological Sciences, R. J. College, Mumbai, Maharashtra, India.

[2]Department of Biological Sciences, R. J. College, Mumbai, Maharashtra, India.

[3]Bombay Veterinary College, Parel, Mumbai, Maharashtra. India

Article Received on
29 April 2014,
Revised on 24 May 2014,
Accepted on 20 June 2014

***Correspondence for Author**
Babita Bhatia
Department of Biological Sciences, R. J. College, Mumbai, Maharashtra, India

ABSTRACT PAGE

The mammalian testis is composed of male germ cells (the gametes) and supporting somatic cells that together promote a highly regulated series of developmental transitions in the seminiferous tubules of the testis to produce functional spermatozoa. Heat is known to cause deleterious effects on the male germ cell line. Mica nanoparticles (nanomica) are known to cure sexual debility, erectile dysfunction, impotency and azoospermia. Under the looming threat of global warming, the aim of the experiment was to substantiate that nanomica can be used as anti-impotency fecundity drug for people living under heat stress conditions. Thirty two male Wistar rats were divided into four groups. G1 acted as control, G2 comprised nanomica only treated group, G3 as heat treated group and G4 were given combined heat treatment and nanomica. The rats were euthanized on day 31 and a small part of the tissue was subjected to ultrastructural study. G1 rats showed normal progression of germ cell development with normal morphological characteristics. G2 rats showed total synchrony in generations of germ cells having normal morphological characteristics, presence of abundant secretory granules and lumen filled with large number of sperms. In G3 rats heat stress had caused degeneration of seminiferous tubules manifested in deleterious changes in somatic and germ cells, undulating basal membrane, apoptotic nucleus and vacuole formation. G4 rats revealed improvement in specific organization of spermatogenic cells, possession of normal morphological characteristics by germ cells, presence of bilayered basal lamina, well defined morphology of sperms and presence of normal Leydig cells. The results indicate that nanomica ameliorates

non-proliferation of germinal epithelium by increasing the specific germ cell associations between developing and proliferating male germ cell line resulting in the formation of normal spermatozoa. Hence, nanomica can evidently be used to improve male reproductive health and to contribute to the therapeutic management of male infertility in heat stressed conditions.

KEY WORDS: nanomica, azoospermia, fecundity, synchrony, apoptotic, therapeutic.

INTRODUCTION

Spermatogenesis is the biological process of gradual transformation of germ cells into spermatozoa, over an extended period of time, within the boundaries of the seminiferous tubules of the testis. Because the tubules are folded repetitively, a cross section of the testis shows several hundred tubule sections, each of which can be identified as one of the stages. [1] The result is that cells of the same developmental stages are seen there in groups. Thus, it is highly improbable that all of the developmental stages will be seen in a single section at the same time. Sequential morphological steps in the precise changes in the *acrosomic system* (a system with prominent granules and hemispherical Golgi apparatus capping the nuclei of a spermatid) differentiation of the spermatids provide the basis for the identification of the stages of the spermatogenic cycle in rats. [2]

Spermatogenesis in rat is a process of gradual transformation of germ cells into spermatozoa over a period of 48-53 days. [3] As the germ cells advance within the seminiferous epithelium, older cells become associated with younger ones in a specific 12 to 13-day cycle that begins with mitotis, proceeds through meiosis and finally ends with the release of sperm. The seminiferous epithelium is composed of four or five of such generations of germ cells. Spermatogenesis is sensitive to various toxic factors (chemical or physical). Some germinal cells (spermatogonia, spermatocytes, spermatids) spontaneously degenerate in the seminiferous tubules of normal individuals.

The germ cell line

It appears as an electron-dense layer, 20-100 nm thick. [4] Basal lamina to be formed of two distinct concentrical layers: basal membrane and lamina propria. [5] The lamina propria consists of three concentric zones:

- the inner zone, *lamina interna* (LI);
- the middle zone, *myoid layer* (ML) consisting of *myoid cells*;

- the outer zone, fibroblast *layer* (FB), consists of fibroblasts and fibrocytes

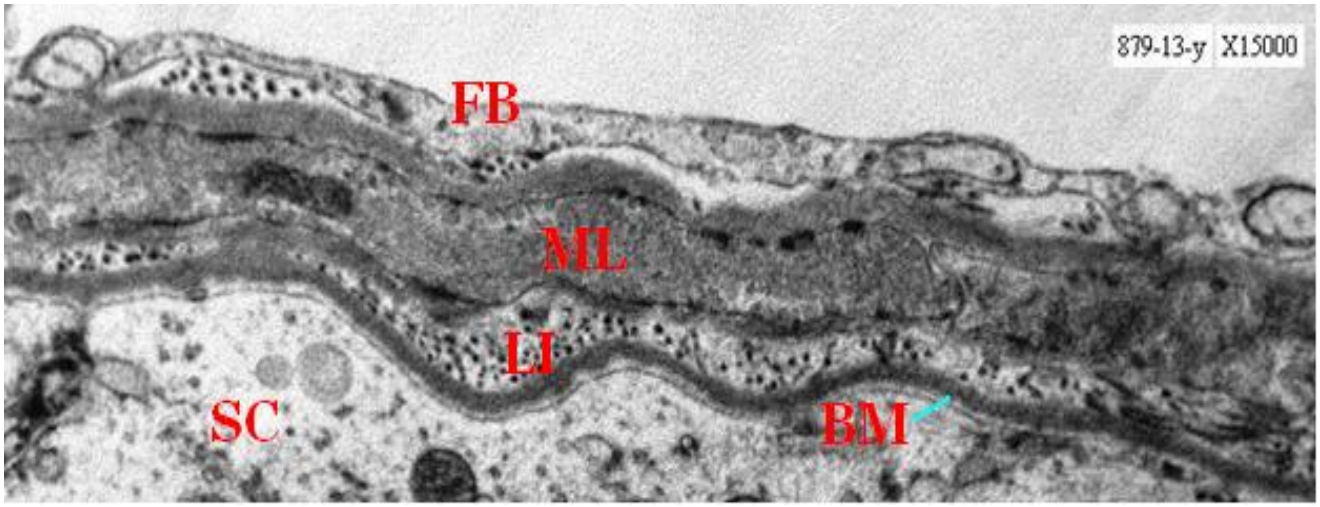

Fig. 1. An electron micrograph of basal lamina of a seminiferous tubule in the testis of a normal rat. (Source: the current study)

The basal lamina provides support to the overlying epithelium, acts as a filter allowing only water and small molecules to pass through and also regulates cell proliferation and differentiation and serves as pathways for cell migration. [6] [7]

Spermatogenic Cells - *the cellular components*

The overall process of spermatogenesis has been variously divided into specific well-defined stages in different species: 6 in human, 12 in mouse, and 14 in rat. [8] [9] [3] The preponderance of cell types can be used for stage identification. In a medical manual it has been outlined spermatogenesis into three distinct phases: [10]

- **Spermatogonial phase** (Mitosis)
- **Spermatocyte phase** (Meiosis)
- **Spermatid phase** (Spermiogenesis)

where spermatogonia (Type-A spermatogonia and Type B spermatogonia), spermatocytes (Primary and Secondary spermatocytes) and spermatids (early round and late elongated Spermatids) are the various cell types comprising the germinal epithelium. Different phases of spermatogenesis and their period of completion is illustrated in Fig.2.

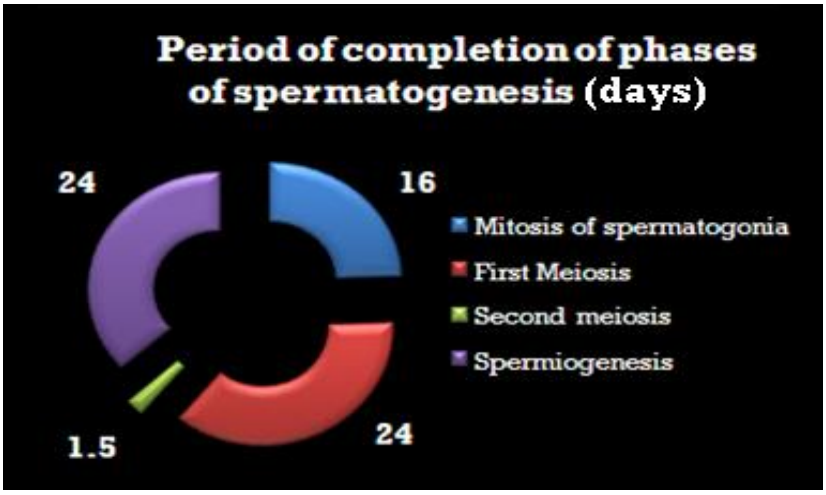

Fig. 2. Different phases of spermatogenesis and the period of their completion.

Hormonal control

The somatic cells (Sertoli cells and Leydig cells) secrete hormones that support the occurrence of normal spermatogenesis. *Luteinizing hormone* (LH) activates the interstitial cells of Leydig to form testosterone. [11] *Follicle Stimulating Hormone* (FSH) stimulates Sertoli cells to manufacture and discharge *androgen-binding protein* (ABP), which binds to testosterone and prevents it from leaving the seminiferous tubule. [12] The increased level of testosterone in the region of spermatogenesis stimulates the process of spermatozoon production.

Alterations in ultrastructure due to heat stress

Classical histological studies in animals have shown that local heating of the testes, whole body heating or surgical induction of cryptorchidism (absence of one or both testes from the scrotum) in rats results in increased death of germ cells (*apoptosis*). [13] Also, mild testicular heating has been established as a safe and reversible approach for suppression of spermatogenesis. [14] Complete recovery of spermatogenesis is by day 56 in rats. [15]

It is well known that duration and period of exposure of the testis to heat determines the nature and severity of the damage induced. Heat stress (43°C) for 15 min induces specific damage limited to spermatocytes whereas 45°C for 15 min results in generalized non-specific damage involving many different germ cell types. [16]

There is reduction in testis mass and slow and incomplete recovery of testis mass after a single heat exposure. [17] Further, these studies revealed that, in rats, heat-induced germ cell degeneration is usually accompanied by alterations in Sertoli cell morphology and functions,

a decrease in rete testes fluid, an increase in serum FSH. Late pachytene primary spermatocytes and early spermatids are the most susceptible to heat. [18]

In heat stressed seminiferous tubules are found vacuoles, highly condensed chromatin and apoptotic bodies in pyknotic nuclei of germ cells. [19] In both Sertoli and spermatid cells mitochondrial degeneration, dilation of smooth endoplasmic reticulum, secondary lysosome formation and enlarged intercellular spaces have been observed in heat stressed animals. [20] Minor sperm chromatin abnormalities and sperm head morphology has been reported in rats subjected to heat stress. [21] Morphological examination of the Leydig cells has recorded accumulation of lipid droplets in the cytoplasm indicating a disturbed steroidogenesis. [22]

MATERIALS AND METHODS

Animals

The current experiment was carried out on 64 healthy adult male albino Wistar rats (150 - 200 g live body weight). They had free access to standard laboratory pellet diet and water *ad libitum.* The animal ethical clearance was obtained from Institutional Animal Ethics Committee (IAEC) approved by Committee for the Purpose of Control and Supervision of Experiment on Animals (CPCSEA)

Incubator

An incubator, based on modern technology, was self-designed to expose rats at a specific temperature while providing good ventilation. It was divided into three compartments, a safety thermostat to maintain a constant temperature of 43^{o}C, a blower and an air ventilator at the top. A state-of-the-art digital microprocess-based controller and an electrical U-shaped concealed rod heater were appropriately placed.

Fig 3. The incubator used for giving heat treatment to one of the group of the experimental rats.

Nanomica

The test drug was procured from a renowned organization, Shree Dhootpapeshwar Ltd, Khetwadi, Mumbai, India, to study its ultrastructural effect on heat-damaged testes. The dose was calculated by extrapolating the therapeutic dose of humans to rat on the basis of BSA ratio (conversion factor 0.018 for rats) by referring to the table of "Paget & Barnes". [23]

Therapeutic dose of nanomica: 15-60 mg

For the experiment, selected human dose: 60 mg

Dose for rats = Human dose x 0.018 = 'X' mg/200g of rat Or, 'X' x 5 = 'Y' g/kg of rat

Therefore, Dose given = 60 x 0.018 = 1.08 mg/200g of rat Or, 1.08 x 5 = 5.4 mg/kg of rat

Vehicle

For the experiments 3 parts of honey was diluted with 4.5 parts de-ionized water and the volume of administration of this freshly prepared diluted honey was 0.5 ml (CCRAS). [24] Each rat was administered their respective doses, as per calculation, vortexed with 0.5 ml diluted honey with an oral gavage.

Grouping of Experimental Animals

Rats were segregated into four groups of eight rats each as follows:

- **Group G1:** served as normal control (standard diet + vehicle)
- **Group G2:** treated with nanomica (nanomica + vehicle)
- **Group G3:** subjected to heat treatment (43^{o}C for 1 hour/daily for 30 days) + vehicle
- **Group G4:** simultaneously given heat and nanomica treatment (heat + nanomica + vehicle)

On day 31, the experimental animals were euthanized by cervical dislocation. For ultrastructural studies, testes of six rats from all the four groups were cut into small pieces (1 mm). The tissue was fixed immediately in 2.5% glutaraldehyde for 6–24 h and then sent to Jaslok Hospital, Mumbai, India, for further processing. The ultra thin sections were mounted on a grid of Transmission Electron Microscope (JEM.1010; JEOL, Tokyo, Japan) and observed under different resolutions. The appropriate testis images in .tiff form were stored.

RESULTS

Distinguishing the cells

To distinguish different testicular cell types, literature survey revealed the following ultrastructural morphological characteristics of germ cells of a normal rat which were used for identification

Sertoli cells: located on the *basal laminae* of the tubuli; extended to the lumen of the tubule; pale**,** large deeply indented nucleus; homogeneous nucleoplasm; a prominent nucleolus; oval mitochondria; a small Golgi apparatus; an agranular endoplasmic reticulum; lipid droplets and lysosomes.

Spermatogonia: located along the basal lamina. Type A spermatogonia - an ovoid nucleus; nucleoli close to the nuclear membrane; electron-dense cytoplasm; a small Golgi apparatus; few mitochondria and many free ribosomes. Type B spermatogonia - rounded nucleus; heavily stained chromatin masses attached to the nuclear membrane and a nucleoli located at the centre of the nucleus.

Primary spermatocyte: large, heterochromatic nuclei located between the basement membrane and the lumen of the tubule. *Secondary spermatocytes*: nuclei are spherical with centrally located clumps of chromatin substance.

Spermatids: differentiated on the basis of the acrosome system. The *early round spermatids* are rounded cells with large spherical nuclei. Lightly stained cytoplasm contains endoplasmic reticulum and mitochondria, which at this stage tend to aggregate at the periphery of the plasma membrane and acrosomic granule. In advanced stages, the *late elongating spermatids* have an eccentric nucleus and the acrosomal cap, elaborated by the Golgi complex, partially covering the nucleus. The mitochondria form a helical arrangement around the proximal flagellum.

Spermatozoa: a typical structure of head, midpiece and tail.

Leydig cells: found adjacent to and in between the seminiferous tubules in the testicle. The mammalian Leydig cells are polyhedral cells with a single eccentrically located ovoid nucleus. [25] The nucleus contains one to three prominent nucleoli and large amount of dark-staining peripheral heterochromatin. The acidophilic cytoplasm usually contains numerous

membrane-bound lipid droplets, large amounts of smooth endoplasmic reticulum, scattered patches of rough endoplasmic reticulum, and several mitochondria.

The electron micrographs of the testis of the experimental rats showed the following ultrastructural features

Ultrastructure of testes of group G1 rats (control)

Fig.4. (a-g) shows that, in the control group (G1) of rats, normal progression of germ cell development has taken place with all the spermatogenic cells showing normal morphological characteristics. Fig 4a depicts normal ***basal lamina (Bl)*** with basal membrane (Bm) and a myoid cell (MC); spermatogenic cells have nucleus (N) with nucleolus (Nu), euchromatin (Eu), heterochromatin (Ht), presence of nuclear membrane (Nm); cytoplasm with cytoplasmic membrane having mitochondria (M), smooth endoplasmic reticulum (SER), rough endoplasmic reticulum (RER), lysosomes (Ly) and cell membrane. The **Sertoli cell (SC)** structure can be identified due to a large nucleus (N) with a slight indentation and marginated heterochromatin (Ht) (Fig. 4b). Its cytoplasmic organelles are well illustrated as a magnified image (x15,000) in Fig. c. The Sertoli cell and spermatogenic cell are separated by intersertoli junctional complex (ISj) (Fig. 4a) and adhering junctions (Aj) (Fig. 4d). **Spermatogonium** is Type-A (SgA) having ovoid nucleus (N) located next to the basal lamina (Bl) (Fig. 4a). The pachytene **primary spermatocyte (pPS)** has large, heterochromatic nuclei (Fig. 4a). A **round spermatid (rSd)** with its normal characteristics can be identified in Fig. 4d due to the peripheral concentration of mitochondrias (M) at one end. Acrosomal formation (As) is evident with well-developed Golgi Apparatus (GA) close to it. A small part of elongating spermatid (egSd) with nucleopores (Np) can be seen in the lower left segment. A cluster of condensing spermatids (egSd) in Fig. 4e are normal as they have a prominent acrosomal cap (Ac) and manchette (Mn), a microtubular structure that assists in elongation. The lumen of the tubule (Lu) is filled with **spermatozoa (Sz)** indicating that the spermatogenesis has gone its normal course (Fig. 4f).

(a)

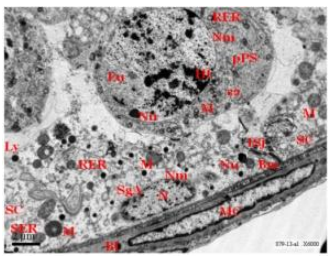

Bl: Basal lamina
Bm: Basal membrane
MC: Myoid cell
SC: Sertoli cell
SgA: Spermatogonia A
pPS: Pachytene Primary Spermatocyte
ISj: Intersertoli cell junction
N: Nucleus
Nu: Nucleolus
Nm: Nuclear membrane
Eu: Euchromatin
Ht:Heterochromatin
M: Mitochondria
SER: Smooth Endoplasmic Reticulum
RER: Rough Endoplasmic Reticulum
Ly: Lysosome

Scale bar = 2µm; Mag. = 6000

(b)

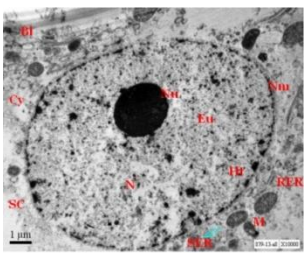

Bl: Basal lamina
SC: Sertoli cell
N: Nucleus
Nu: Nucleolus
Nm: Nuclear membrane
Eu: Euchromatin
Ht:Heterochromatin
Cy: Cytoplasm
M: Mitochondria
SER: Smooth Endoplasmic Reticulum
RER: Rough Endoplasmic Reticulum

Scale bar = 1µm; Mag. = 10000

(c)

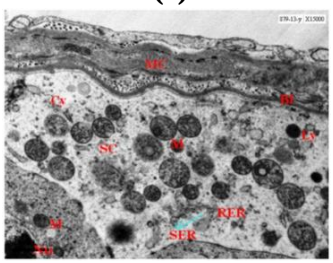

Scale bar = 2µm; Mag. = 15000

(d)

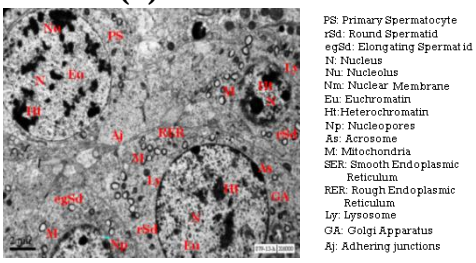

Scale bar = 2µm; Mag. = 6000

(e)

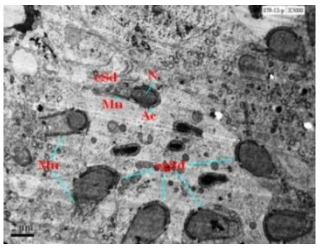

Scale bar = 2µm ; Mag. = 5000

(f)

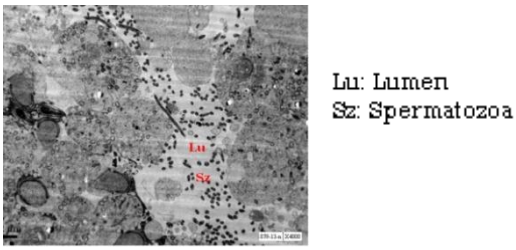

Scale bar = 2µm; Mag . = 400

(g)

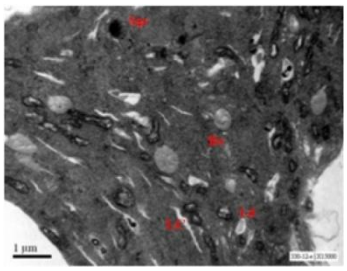

Scale bar = 1µm; Mag. = 15000

Fig. 4. Electron micrographs of cross sections of testes of control group of rats (G1), each showing part of a seminiferous tubule

Interstitium contains **Leydig cells (LC)** characterized by their round nucleus, blood vessels (Bv), secretory granules (Sgr) and a lipid droplet (Ld) (Fig. 4g).

Ultrastructure of testes of Group G2 rats (nanomica treated)

This group was given nanomica with honey and the ultrastructural characteristics of the testis of rats in this group were as follows Fig. 5 (a-f) depicts **seminiferous tubules** of nanomica administered rats showing proliferation of germ cells as evident from large number of spermatozoa in the lumen of the tubules (Fig. 5e). In the tubule there are 4 generations of

germ cells developed in total synchrony with one another and all show normal morphological characteristics (Fig. 5a). The germ cells are arranged in discrete layers on thin basal lamina (Bl) (Fig.5a). These spermatogenic cells are supported by the cytoplasmic (SCcy) processes of the Sertoli cell (SC). All the germ cells are at their specific locations.

The **remarkable features** of this set of sections are presence of abundant secretory granules (Sgr) indicating an active secretory state and a crescent shaped vacuole (V) in the cytoplasm of **Sertoli cell** (Fig. 5a). Clearly visible intra-Sertoli cell junctions (ISj) can be noticed (Fig. 5a). Type-B spermatogonium (SgB) is identified by the ovoid nucleus and centrally placed nucleolus (Nu) (Fig. 5b). Two **Type-B spermatogonia (SgB)** are connected through the intercellular bridge (Fig. 5a). **Primary spermatocytes (PS)** are in the beginning of diakinesis stage characterized by shortening and thickening of the chromatin in Fig. 5a while **primary spermatocyte (PS)** is in the anaphase I stage in Fig. 5b as the v-shaped chromatids are seen to be pulled towards the opposite poles. They are in the process of differentiation to round **spermatids.** In the cytoplasm (Cy) of these primary spermatocytes, the mitochondrias (M) are seen to be migrating towards the periphery of the cell. Elongated spermatids (eSd) have a distinct acrosomal cap (Ac) at the anterior end and manchette structure (Mn) at the tail end (Fig. 5d). Lumen (Lu) is filled with large number of **sperms (Sz)** which, when comparing to control animals, indicates that the drug enhances sperm number (Fig. 5e).

(a)

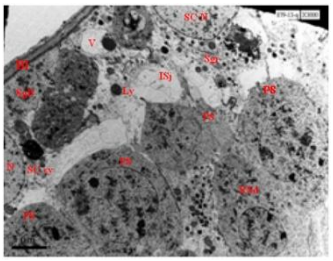

Bl: Basal Lamina
SC: Sertoli cell
SgB: Spermatogonia B
PS: Primary Spermatocyte
RSd: round Spermatid
ISj: Intrasertoli cell Junction
N: Nucleus
Cy: Cytoplasm
Sgr: Secretory Granules.
V: Vacuole

Scale bar = 1µm; Mag. = 3000

(b)

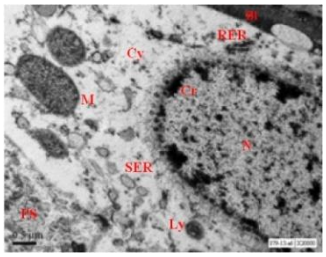

Bl: Basal Lamina
PS: Primary Spermatocyte
N: Nucleus
Cr: Chromatin
Cy: Cytoplasm
M: Mitochondria
SER: Smooth Endoplasmic Reticulum
RER: Rough Endoplasmic Reticulum
Ly: Lysosome

Scale bar = 1µm; Mag. = 20000

(c)

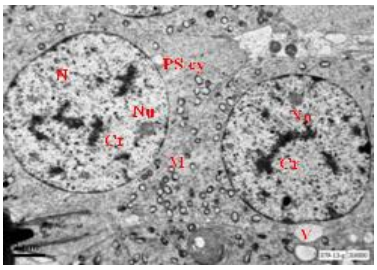

PS: Primary Spermatocyte
N: Nucleus
Nu: Nucleolus
Cr: Chromatin
Cy: Cytoplasm
M: Mitochondria
V: Vacuole

Scale bar = 2µm ; Mag. = 6000

(d)

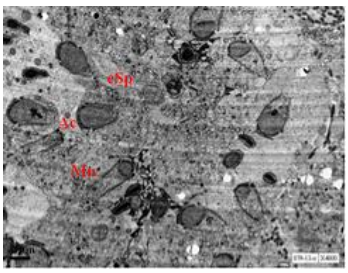

eSd: Elongated Spermatid
Ac: Acrosomal cap
Mn: Manchette

Scale bar = 2µm; Mag. = 4000

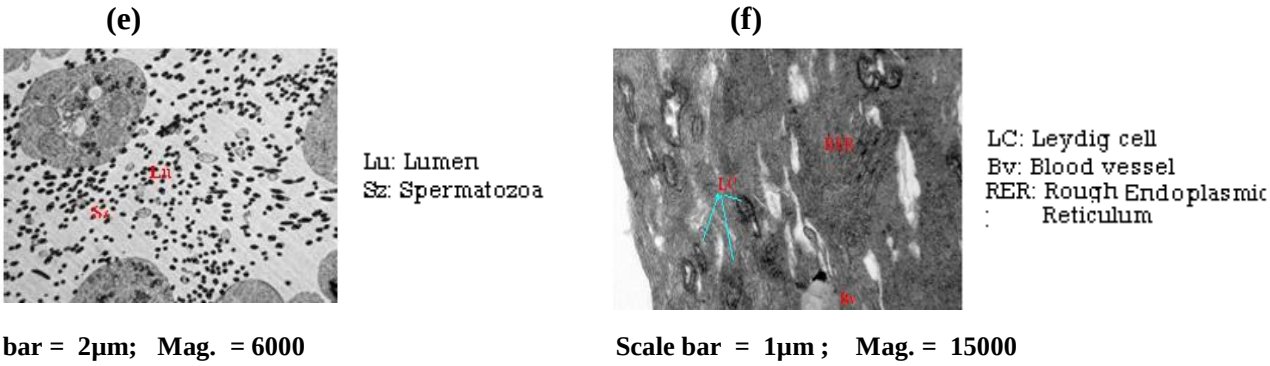

Fig. 5. (a-f) Electron micrographs of cross sections of testes of nanomica treated group of rats (G2), each showing part of a seminiferous tubule

The other **common and normal characteristics** of the germ cells are that they have typical nucleolus (Nu) and chromatin (Cr) in the nucleus; mitochondria (M), smooth endoplasmic reticulum (SER), rough endoplasmic reticulum (RER) and lysosomes (Ly). The **Leydig cells** (LC) with characteristic oval shape, a blood vessel (bv) and rough endoplasmic reticulum (RER) are distinctly identified in the Interstitium.

Ultrastructure of testes of group G3 rats (heat treated)

Different degrees of damage to seminiferous tubules were noted in the heat treated rats. Heat stress had caused alterations in spermatogenic cycle that were not seen in rats not subjected to heat stress. The morphological features of the seminiferous epithelium in heat-treated rats are shown in Fig. 6 (a-j).

It is apparent from these figures that the placement of germ cells and the synchronization of germ cell development (the cycle of seminiferous epithelium), increasingly disorganized, is evident from this set of images. The **basal membrane** has lost its normal contour and is wavy or undulating with basal lamina (Bl) appearing almost torn with gap with undefined myloid cell (Fig. 6 and Fig. 6c). The **germ cells** have lost their original position and are dislocated as the germ cells can be seen sloughed off from the basal lamina losing the continuity with the membrane (Fig. 6 and Fig. 6c). **Sertoli cell (SC)** is dislocated from the basal portion (Fig. 6b) and a **late spermatid (lSd)** is inappropriately placed close to the Sertoli cell nucleus (Fig. 6a). The cytoplasmic organelles like mitochondria (M) have ventured out from the cytoplasm into the testicular parenchyma. (Fig. 6a and Fig.6c). As a result the cytoplasm of the germ cells lacks any organelles in them.

The cells are found to be apoptotic as the **nucleus (N)** of the cells has lost its nuclear membrane or has become discontinuous. The nucleus has undergone condensation into (pyknosis), a hallmark of apoptosis (Fig. 6a and Fig. 6c). Nuclear contents are poorly defined as euchromatin and heterochromatin cannot be distinguished due to apoptosis, which has led to condensation of chromatin (Cr) (Fig. 6c). The **cytoplasm (Cy)** has become dense and the cell shows vesicles called *apoptotic bodies* (Ab) and vacuole formation (V) (Fig. 6a**).** Apoptosis is characterized by a series of typical morphological features, such as shrinkage of the cell, fragmentation into

(a) **(b)** **(c)**

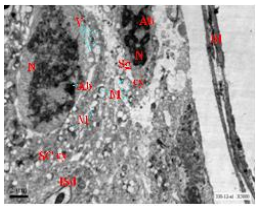

Bl: Basal Lamina
SC: Sertoli cell
Sg: Spermatogonia
Sd: Spermatid
N: Nucleus
Ab: Apoptotic Body
Cy: Cytoplasm
M: Mitochondria
V: Vacuole

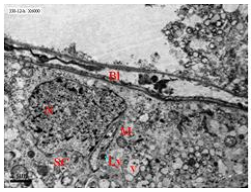

Bl: Basal lamina
SC: Sertoli cell
N: Nucleus
M: Mitochondria
Ly: Lysosome
v: Vacuole

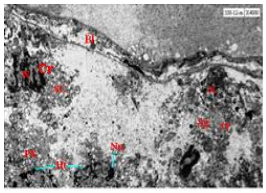

Bl: Basal lamina
SC: Sertoli cell
Sg: Spermatogonia
PS: Primary Spermatocyte
N: Nucleus
Nu: Nucleolus
Cr: Chromatin
Ht:Heterochromatin
Cy: Cytoplasm

Scale Bar = 2 µm ; Mag. = 6000 **Scale Bar = 2 µm; Mag. = 6000** **Scale Bar = 2 µm; Mag. = 4000**

(d) **(e)** **(f)**

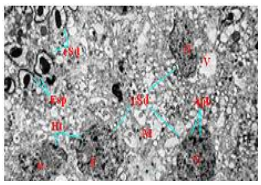

eSd: Elongated Spermatids
rSd: Round Spermatid
Apb: Apoptotic bodies
Esp: Ectoplasmic specialization
N: Nucleus
Ht:Heterochromatin
M: Mitochondria
V: Vacuole

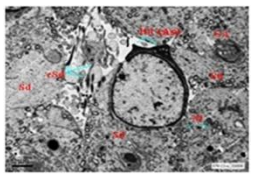

Sd: Spermatid
eSd: Elongated Spermatids
M: Mitochondria
Hd(As): Acrosome system
GA: Golgi Apparatus

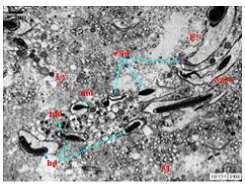

eSd: Elongated Spermatids
Szoo: Spermatozoon
ES: Ectoplasmic Specialization
M: Mitochondria
hd: Head piece
md: Midpiece
Ly: Lysosome

Scale Bar = 2 µm ; Mag. = 4000 **Scale Bar = 1 µm; Mag. = 30000** **Scale Bar = 2 µm; Mag. = 4000**

(g) **(h)** **(j)**

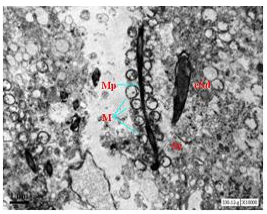

eSd: Elongated Spermatid
Sz: Spermatozoa
Mp: Mid piece
M: Mitochondria

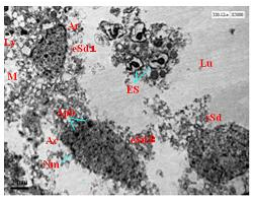

eSd1, eSd2: Elongated Spermatid
rSd: Round Spermatid
ES: Ectoplasmic Specialization
Nm: Nuclear Membrane
M: Mitochondria
Ly: Lysosome
Ac: Acrosome System
Apb: Apoptotic bodies
Lu: Lumen
Ar: Acrosomal ring

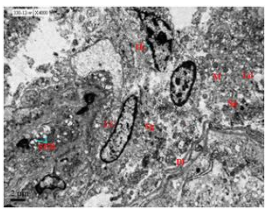

LC: Leydig Cell
M: Mitochondria
SER: Smooth Endoplasmic Reticulum
Sg: Secretory granules
Bl: Basal lamina
Ld: Lipid Droplet

Scale Bar = 1 µm Mag. = 10000 **Scale Bar = 2 µm; Mag. = 5000** **Scale Bar = 2 µm; Mag. = 4000**

(iα) **(iβ)** **(iδ)**

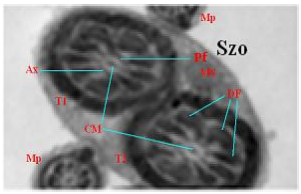

T1: Tail
T2: Tail
Mp: Mid Piece
MS: Mitochondrial Sheath
DF: Dense Fibres
Ax:Axonemal Complex
Pf:Peripheral microtubules
CM: Central Microtubules

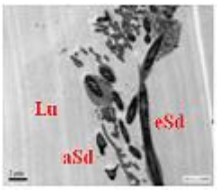

Lu: Lumen
aSd:Abnormal Spermatid
eSd: Elongated Spermatid

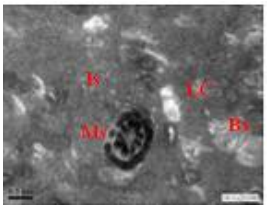

Is: Interstitium
Ms: Mitochondrial Sheath
LC: Leydig Cell
Bv: Blood vessel

Scale Bar = 0.5 µm; Mag. = 30000 **Scale Bar = 2 µm; Mag. = 6000** **Scale Bar = 0.5 µm; Mag. = 25000**

Fig. 6 (a-j). Electron micrographs of cross sections of testes of heat treated rats (G3), each showing a part of a seminiferous tubule

membrane-bound apoptotic bodies and rapid phagocytosis by neighbouring cells. The cytoplasmic organelles can be seen deformed or are totally absent.

Mitochondria are vacuolated, with degenerated cristae are visible in all the plates. Type of spermatogonia, spermatocyte and spermatid is very difficult to distinguish as pyknosis has occurred in the nucleus which has condensed and cytoplasm has merged with the testicular parenchyma, losing all its organelles. However, spermatids can be identified due to the alignment of mitochondria at one end of the cell membrane which is the characteristic feature of spermatids. (Fig. 6c and 6d). Differentiation of few elongated spermatids (eSd) appeared in the last stage of spermiation in which the cell is seen to be arrested. (Fig. 6 a-f and Fig. 6g).

Some of the features evident in the sections in this study were quite noteworthy. **Spermatogonia** (Sg) are showing crenated nucleus (N) as it has undergone shrinkage and have acquired a notched or scalloped surface (Fig. 6a). **Sertoli cell (SC)** shows fragmentation with a single indentation dividing it into two halves (Fig. 6b). The nucleus of **spermatids (rSd)** has taken "bead-like" appearance (Fig. 6d). Partially preserved ectoplasmic specialization (Esp) is noticed in spermatids (Fig. 6d). Nucleus of an abnormal developing spermatid (abSd) is seen with two acrosome system (As), likely to differentiate into a spermatozoa with two heads (Hd) (Fig. 6e). The **sperms** have attained an abnormal morphology due to heat treatment is proven in the set of images in Fig. 6 (iα-iδ) in which (Fig. 6 iα) shows transverse section of an abnormal spermatozoa (Szo) with mid-pieces of two tails (T1 and T2) that are surrounded by a mitochondrial sheath (MS). Each tail has an axonemal complex (Ax), consisting of two central (CM) and nine paired peripheral (Pf) microtubules. The axial microtubules are enclosed within outer dense fibres (DF). Two small parts of transverse section of main-piece (Mp) of two tails can be seen adjacent to Szo, on the either side. The Fig. 6 iβ shows longitudinal sections of elongated spermatids (eSd) and 1 or 2 abnormal spermatids (aSd) in the lumen (Lu) of a tubule. The Fig. 6 iδ) shows abnormal mid-piece of a tail with disrupted mitochondrial sheath (Ms) in the interstitium (Is) with 2-3 Leydig cells (LC) and a blood vessel (Bv).

Other features visible are a well defined Golgi apparatus (GA) in the cytoplasm of a spermatid (Sd) (identified due to alignment of mitochondrias at one end), marked in the (Fig. 6e). In Fig. 6f **elongating spermatids (eSd)** at various stages of differentiation can be observed. In some of these spermatids only head (Hd); in two of the spermatids midpiece

(Mp), and in one spermatid fully grown spermatozoon (Szoo) tail can be identified. This spermatozoon shows a typical head, mid-piece and tail. Ectoplasmic specialization (ES) can be clearly distinguished and lysosomes (Ly) are strewn all over the testicular parenchyma. Longitudinal section of the middle piece of developing **spermatozoa** showing longitudinal alignment of mitochondrias (M) along the mid piece can be seen in Fig. 6g. In the Fig. 6h**,** apoptotic **spermatids (rSd, eSd1, eSd2)** have been sloughed off into the lumen of seminiferous tubule. Two apoptotic bodies (Apb) can be identified. These spermatids seem to have lost their development during the process of spermiation and no spermatozoa could be seen in the lumen, which is an important observation for this study. The Fig. 6j depicts vacuolated interstitium with few **Leydig cells (LC)**, one of which shows distorted nucleus (N). Large amount of dark-staining peripheral heterochromatin (Ht) is well defined in each LC. In the cytoplasm, smooth endoplasmic reticulum (SER) and swollen mitochondria (M) can be distinguished. A part of wavy basal lamina (Bl) can also be seen in this section.

Ultrastructure of testes of group G4 rats (heat- nanomica treated)

Even after heat treatment, all stages of sperm development were visible within the seminiferous epithelium of most of the tubules. However, in very few the placement of germ cells and the synchronization of germ cells development was found disorganized while few were found to be in the recovery stage as the tubules showed both normal and abnormal characteristics. The ultrastructure observed in these three different types of tubules observed in the heat- nanomica treated group of rats are as follows

Fig. 7 (a-k) are sets of images of the cross sections of **seminiferous tubules** that indicates the presence of normal seminiferous tubules in heat- nanomica treated group (G4) of rats. The tubules are covered by thin basal lamina (Bl) and spermatogenic cells organized in the specific manner. The germ cells are localized at their appropriate places and possess normal morphological characteristics. The nuclear membrane and the cell membrane are intact in all the germ cells.

(a)

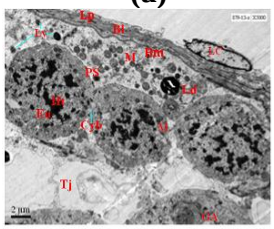

Bl: Basal lamina
Bm: Basal membrane
LC: Leydig Cell
PS: Primary Spermatocyte
Lp: Lamina Propria
Tj: Tight Junctions
Cyb: Cytoplasmic Bridge
M: Mitochondria
Ht:Heterochromatin
Eu: Euchromatin
Ly: Lysosome
GA: Golgi Apparatus
Ld: Lipid Droplet

Scale Bar = 2µm; Mag. = 5000

(b)

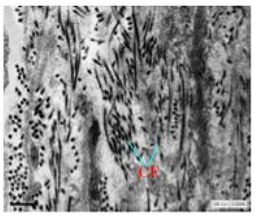

CF: Collagen Fibres

Scale Bar = 0.5µm; Mag. = 30000

(c)

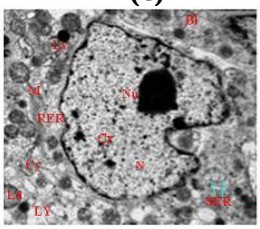

Bl: Basal lamina
N: Nucleus
Nu: Nucleolus
Cr: Chromatin
Cy: Cytoplasm
M: Mitochondria
RER: Rough Endoplasmic Reticulum
SER: Smooth Endoplasmic Reticulum
Ly: Lysosome
GA: Golgi Apparatus
Ld: Lipid Droplet

Scale Bar = 2µm; Mag. = 10000

(d) **(e)** **(f)**

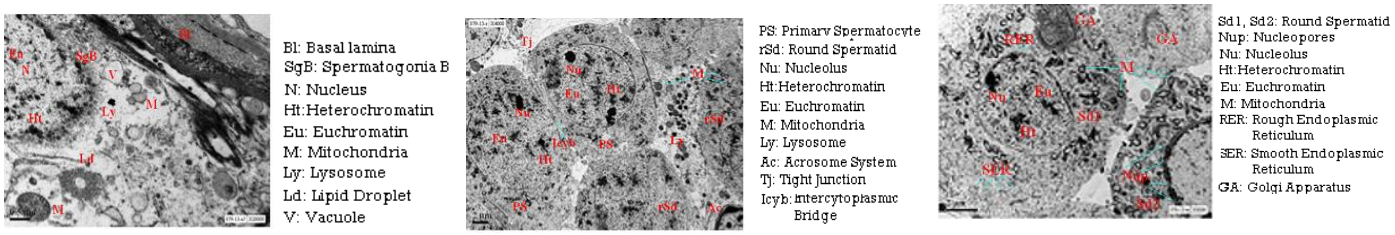

Scale Bar = 0.5µm; Mag. = 20000 **Scale Bar = 2µm; Mag. = 4000** **Sscale Bar = 2µm; Mag. = 8000**

(g) **(h)** **(i)**

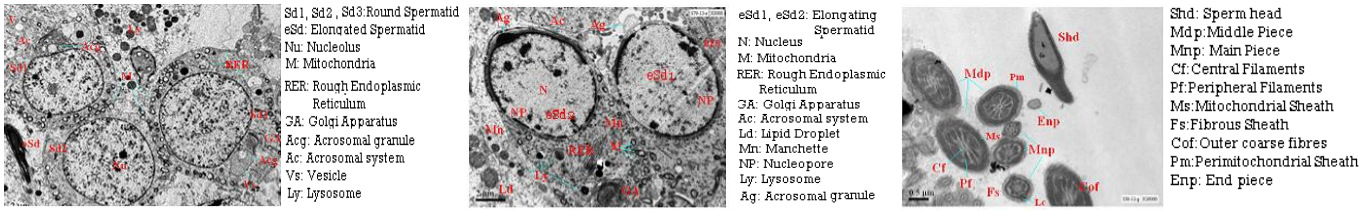

Scale Bar = 2µm; Mag. = 6000 **Scale Bar = 2µm; Mag. = 8000** **Scale Bar = 0.5µm; Mag. = 20000**

(j) **(k)**

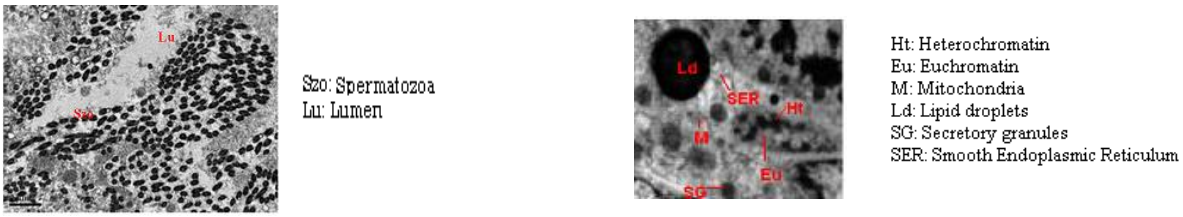

Scale Bar = 2µm; Mag. = 2000 **Scale Bar = 0.5µm; Mag. = 20000**

Fig.7 (a-k). Electron micrographs of cross sections of testes of heat- nanomica treated rats (G4), each showing a normal seminiferous tubules inspite of heat treatment

The noteworthy features of these sections have been that **basal lamina (Bl)** is formed of two distinct concentrical layers: basal membrane (Bm) and lamina propria (Lp). The basal membrane is in contact with the seminiferous epithelium. Intersertoli cells junction, the tight junction (Tj), is clearly evident in Fig. 7a. The inner zone of lamina propria, adjacent to the basement membrane, contains large amounts of collagen fibre (CF) (Fig. 7b). **Type-A spermatogonia** can be seen lying close to the basement membrane. This spermatogonium has ovoid nucleus (N) with euchromatin (Eu) filling the whole nucleus and marginated heterochromatin (Ht) (Fig. 7d). Two normal **primary spermatocytes (PS)** linked by inter-cytoplasmic bridges (Icyb) are seen to be present in the Fig. 7e. Fig. 7f depicts two **round spermatids Sd1 and Sd2**. Sd1 which is an early spermatid show normal nuclear structure with nuclear membrane, euchromatin, heterochromatin and nucleolus. Its cytoplasm consists of rough endoplasmic reticulum, very prominent Golgi apparatus and several mitochondrias

with distinct cristae. Sd2 is round spermatid showing nuclear pores (Np). The Fig. 7g shows early differentiating spermatid (Sd1 and Sd3) with acrosomal system (Ac).

Ac has a small proacrosomal granule (Ag) in the centre which is seen to be attached to the nucleus. These granules appear to be surrounded by a vesicle (Vs). Sd2 is also a normal round spermatids having normal nuclear and cytoplasmic structure. The Fig. 7h intermediate spermatid (iSd) seems to have an oval nucleus in acrosomal phase as it contains acrosomal granule at one end, one-third of the nucleus covered by the acrosomal cap (Ac) and nuclear pores (Np) in the rest of the nuclear membrane. The shape of nucleus (N) appears to be turning from spherical to ovoid, while in the cytoplasm, it is noticed that mitochondrias (M) have migrated towards the caudal pole of the cell, opposite the acrosomal system. Manchette structure (Mn) is obvious in the caudal part of the cell**.** A cross-section of the main pieces (Mnp), middle piece (Mdp) and an end piece (Enp) of **sperm** tail and a section through one sperm head (Shd) in the lumen of the tubule appear well defined (Fig. 7i). The axial filament consists of two central (Cf) and nine paired peripheral filaments (Pf). The outer coarse fibers (Cof) and the fibrous mitochondrial sheath (Ms) surround the axial filaments. Increased output of sperms (Sz), due to nanomica treatment, is evident due to the presence of large number of sperms in the lumen (Lu) of the tubule (Fig. 7j).

In the Fig. 7c the other normal and expected features were that the **Sertoli cell** nucleus (N) shows indentation of the nuclear membrane. Prominent nucleolus (Nu) and chromatin material (Cr) occupy the nucleoplasm. The **germ cell** cytoplasm (Cy) contains numerous mitochondrias (M) with cristae, distinct Golgi apparatus (GA), smooth endoplasmic reticulum (SER), rough endoplasmic reticulum (RER), lysosomes (Ly) and lipid droplets (Ld). The **spermatids** of these sections show normal mitochondrias (M) which appear to be moving towards one pole of the cell, rough endoplasmic reticulum (RER), Golgi Apparatus (GA) and acrosomal granule (Ag). A normal **Leydig cell** nucleus (N) has euchromatin (Eu) and peripheral heterochromatin (Ht) as seen in Fig. 7k. It also shows that its cytoplasm contains mitochondrias (M), smooth endoplasmic reticulum (SER), secretory granules (SG) and a lipid droplet (Ld).

The set of images, Fig. 8 (a-f), are of the cross sections of seminiferous tubules from which it can be deciphered that the tubules are in the recovery stage as the germ cells comprising them possess both normal and altered morphologies. The **Sertoli cell** is showing an irregularly shaped nucleus (N). However, the nucleus contains a prominent nucleolus (Nu),

euchromatin (Eu) and heterochromatin (Ht) which is normally found in them. The cytoplasmic organelles and both nuclear and cell membrane are well defined unlike the completely degenerated tubules where they undergo apoptosis. The mitochondria are found to be swollen (Fig. 8a). A section (Fig. 8b) shows both a normal **primary spermatocyte (PS)** and an adjacent abnormal spermatid (abSd), whose nucleus (N) has lost its normal contour. Its cell membrane has lost its natural shape and is broken from one side. The cytoplasmic organelles have got dispersed in the testicular parenchyma. However, it has swollen mitochondria (M), abnormally placed but normal Golgi apparatus (GA) and abundant rough endoplasmic reticulum (RER). Both swollen mitochondria (sM) and mitochondrias with degenerated cristae (cM) are present in the testicular parenchyma (Fig. 8c). In Fig. 8d a few **round spermatids (rSd)** with normal nucleus in the nucleopore (Np) stage show lots of vacuoles, swollen mitochondria (sM) and lysosomes (Ly) in their cytoplasm which is quite abnormal. Also, the abnormal elongated spermatids (eSd) with their development arrested, occupy the lumen (Lu) and dead spermatozoa seem to be sloughed off from the germinal epithelium (Fig. 8**d**) forming the cell debris. In one of the tubules both normal and abnormal round spermatids in different stages of differentiation are seen (Fig. 8**e**). A round spermatid (rSd1) in the acrosome phase with acrosome cap (Ac) on the nuclear envelope is present while in the rest (rSd2 and rSd3) acrosome has completely flattened on the nuclear membrane and the nucleus has taken an abnormal shape.

(a)

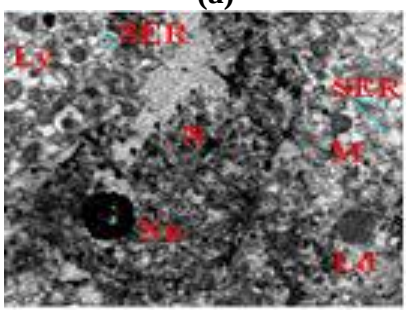

N: Nucleus
M: Mitochondria
Nu: Nucleolus
SER: Smooth Endoplasmic Reticulum
Ld: Lipid Droplet
Ly: Lysosome

Scale Bar = 0.5µm; Mag. = 10000

(b)

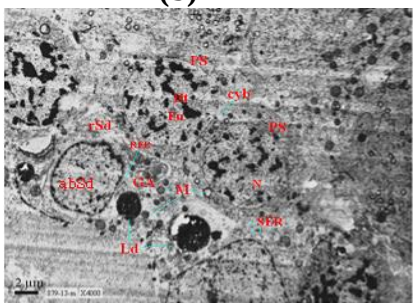

rSd: Round Spermatid
abSd: Abnormal Spermatid
PS: Primary Spermatocyte
N: Nucleus
Ht:Heterochromatin
Eu: Euchromatin
Nu: Nucleolus
M: Mitochondria
SER: Smooth Endoplasmic Reticulum
Ld: Lipid Droplet
GA: Golgi Apparatus
cyb: Cytoplasmic Bridge

Scale Bar = 2µm; Mag. = 4000

(c)

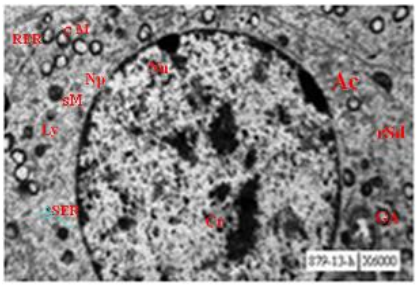

rSd: Round Spermatid
Nu: Nucleolus
Cr: Chromatin
Np: Nucleopores
Ac: Acrosome System
sM: Swollen Mitochondria
cM: Mitochondria with degenerated cristae
Ly: Lysosomes
RER: Rough Endoplasmic Reticulum
GA: Golgi Apparatus

Scale Bar = 2µm; Mag. = 6000

(d)

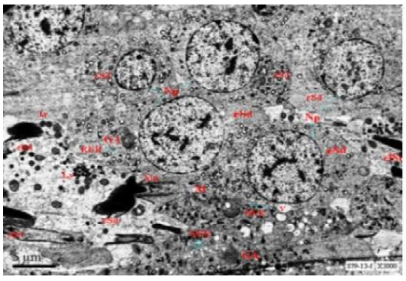

rSd: Round Spermatid
eSd: Elongated Spermatids
Np: Nucleopores
SER: Smooth Endoplasmic Reticulum
RER: Rough Endoplasm Reticulum
GA: Golgi Apparatus
Mn: Manchette
M: Mitochondria
Ly: Lysosomes
v: Vacuole

Scale Bar = 5µm; Mag. = 3000

(e) **(f)**

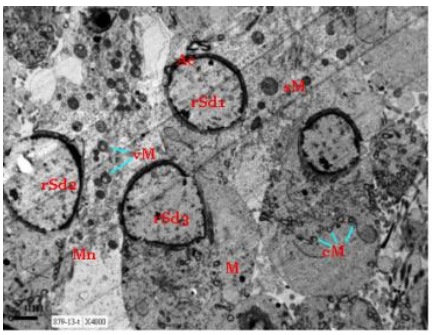

rSd1,rSd2,rSd3: Round Spermatid
Ac: Acrosome system
M: Normal Mitochondria
vM: vacuolated mitochondria
cM: Mitochondria with degenerated cristae
sM: swollen Mitochondria
Mn: Manchette

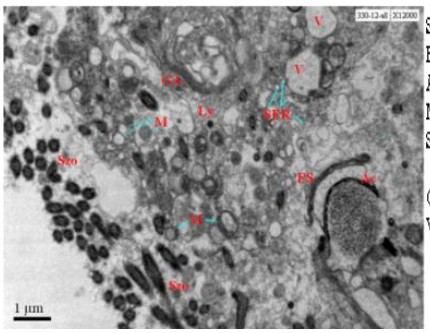

Szo: Spermatozoa
ES: Ectoplasmic Specialization
Ac: Acroisome System
M: vacuolated Mitochondria
SER: Smooth Endoplasmic Reticulum
GA: Golgi Apparatus
V: Vacuole

Scale Bar = 2µm; Mag. = 4000 **Scale Bar = 1µm; Mag. = 12000**

Fig. 8(a-f). Electron micrographs of cross sections of testes of heat- nanomica treated rats (G4), each showing part of a seminiferous tubule recovering from heat stress

However, alignment of the mitochondria (M) at the caudal pole (Fig. 8e) and manchette formation (Mn) (Fig. 8d) appears to be normal.. The testicular parenchyma is degenerated with vacuolated mitochondria (vM), swollen mitochondria (sM), and mitochondrias with degenerated cristae (cM), Golgi apparatus (GA), lysosomes (Ly), vacuoles (V) and smooth endoplasmic reticulum (SER). An abnormal elongated spermatid (eSd) in acrosomal phase can be seen with acrosomal cap (Ac), ectoplasmic specialization (ES) and an abnormally shaped nucleus (N) (Fig. 8f)**.** However, the TS of **spermatozoa (Szo)** in the lumen and few in the parenchyma appear to be normal (Plate Fig. 8**f).**

The ultrastructure of tubular sections of few heat- nanomica treated animals in the Fig. 9 (a-i) have completely degenerated tubules indicating that nanomica has been unable to produce any amelioration after heat treatment in these tubules. The **basal lamina (Bl)** is irregular, swollen with gaps, the layers are not well defined and devoid of myoid cells (Fig. 9a). The basal lamina shows a lipid droplet in Fig. 9c. **Sertoli cells (SC)** (Fig. 9c), **Type-A spermatogonia** (round nucleus) (SgA), **Type-B spermatogonia** with dense nucleus showing euchromatin (Eu) and heterochromatin (Ht) can be distinguished. There are two more germ cells with round nucleus and no nuclear membrane, cell membrane and cytoplasmic organelles are visible. However, they could not be identified as spermatocytes and round spermatids as they are completely apoptotic. Since the nuclear membrane and cell membrane are not well defined, the cytoplasmic organelles have ventured out into the Sertoli cell cytoplasm (Fig. 9a). Abnormal placement of the growth-arrested **elongated spermatid (eSd)** near the basal lamina (Bl) (Fig. 9b and Fig. 9d). and also abnormally placed primary spermatocyte near the basal lamina in the image (Fig. 9b) is noteworthy. **Leydig cells** show

hypertrophy with enlarged and elongated nucleus and darkly stained cytoplasm in which are present swollen mitochondrias (sM), and collagen fibres (Cf) (Fig. 9**i**). The salient features of these sections are that Sertoli cell nuclei is pyknotic, irregularly shaped, with clumped chromatin (Cr) and disrupted nuclear membrane (Nm) (Fig. 9**c**). Vacuolated mitochondria (vM) and vacuoles (V) can be identified in the Sertoli cell cytoplasm. Both swollen (sM) and vacuolated (vM) are present in apoptotic round spermatid (rSd) (Fig. 9**d**). An apoptotic early round spermatid (eSd) with irregular, discontinuous nuclear membrane can be identified because of the alignment of swollen mitochondria at one end of the cell (Fig. 9**e**). The Fig. 9**h** shows abnormal elongated spermatid cells (eSd1 and eSd2) in the upper segment of the section. The head (Hd) of eSd1 has a with disrupted acrosomal cap (Ac) and a surrounding

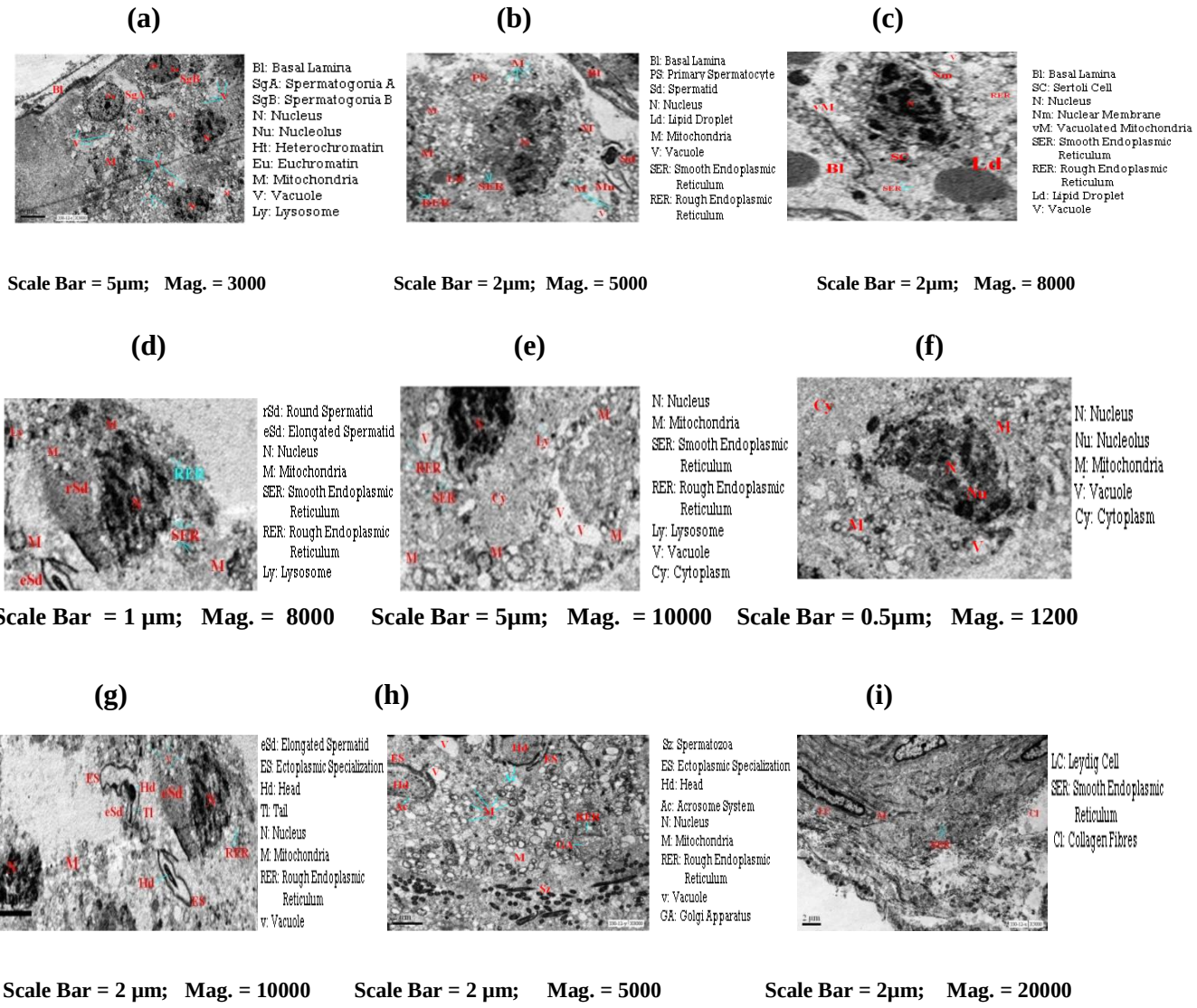

Fig. 9(a-i). Electron micrographs of cross sections of testes of heat- nanomica treated rats (G4), each showing completely degenerated seminiferous tubules caused due to heat treatment.

Ectoplasmic specialization (ES). The early spermatid eSd2 has an abnormally shaped head (Hd) surrounded by ES. An abnormal spermatid, which has taken spiral shape is a unique feature of this study and perhaps not been reported before (Fig. 9f). It is identified due to the alignment of the mitochondria along the periphery of the cell. An elongated spermatid (eSd) with deformed ectoplasmic specialization (ES), a head and the flagellum of a developing spermatozoon forms a part of these set of images (Fig. 9g). Next to it, an elongated spermatid (eSd), can be seen with only the head of the spermatozoon and ectoplasmic specialization (ES) surrounding it. However, the development of **spermatozoon** is arrested.

The other features that are identified from these sections are that the **testicular parenchyma** is highly vacuolated with lots of vacuolated mitochondria (vM) and mitochondria with degenerated cristae (cM). The **germ cells** have cytoplasm comprising smooth endoplasmic reticulum (SER), rough endoplasmic reticulum (RER), Golgi apparatus (GA), lysosomes (Ly), lipid droplets (Li) and vacuoles (V). TS and LS of spermatozoa (Sz) can be observed in (Fig. 9h). An elongated spermatid (eSd), in which differentiation into spermatozoa is arrested, can be identified (Fig. 9d).

DISCUSSION

Hyperthermia is shown to be closely associated with oxidative stress, followed by apoptosis of germ cells. [26] Hyperthermia, the mitochondrial degeneration, dilatation of smooth endoplasmic reticulum and enlarged intercellular spaces are observed in both Sertoli and spermatid cells. The damaging effects of whole body or local heating on the testes of mammals are well known and, although recovery begins about 40 days after a single exposure, even 60 or more days later, a significant reduction in testis mass. Exposure to heat can produce testicular atrophy, spermatogenetic disruption and changes in germ cell morphology. Extending these earlier morphological findings, our present study clearly demonstrates that apoptosis is the underlying mechanism of heat-induced (43^{o}C for 1 h) germ cell death in the adult rat. Heat results in an enhanced production of reactive oxygen species (ROS) in cells/tissues and exert oxidative stress (OS), which in turn, increases the rate of cellular damage.

Oxidative injury to cell membranes leads to major ionic imbalance, mitochondrial damage, and then activation of lysosomes. [27] An important role of basement membrane is maintaining the integrity of tissues. Basement membrane can stabilize the structure of tissue and sends signals to the cells. Some reports have shown that certain exogenous stimulants may induce

myoid cells to produce more collagen and ECM that are responsible for thickness of basal lamina. Therefore, it may increase thickness of the basement membrane and change its appearance to irregular, wavy, multilaminar shape.

The characteristic response of Sertoli cells to heat-induced testicular damage is the accumulation of lipid droplets and dense bodies in its cytoplasm. The formation of large amounts of lipids within Sertoli cells can be attributed to the phagocytosis and breakdown of degenerated germ cells. [28] A similar explanation seems likely in the present study. Similar prominence of phagocytic activity by Sertoli cells was noted in rats treated with heat (G3) that caused degeneration of spermatocytes and spermatids. An interesting suggestion has been made that that phagocytosis of lipids may stimulate the Sertoli cell to synthesize a substance (steroid?) capable of influencing spermatogenesis, thus playing a part in the regulation of cyclic activity in the seminiferous tubules. [29] Observation of detached germ cells, abnormal sperms, and mislocation of spermatids and spermatozoa to positions that are closely related to the basement membrane may be due to the rapid disruption of Sertoli-germ cell interaction. [30] These investigators have also suggested that this physical interaction ultimately leads to the sloughing of the germ cells from the seminiferous epithelium.

It has been clear for some time that the most sensitive cells in the testes are the pachytene primary spermatocytes. Pachytene spermatocytes, dividing spermatocytes and early spermatids have been found to be the most frequent cell type observed undergoing apoptosis while spermatogonia are relatively heat resistant. [31] The response of these cells to heat is rapid and there is histological damage within 1-12 h after heating, indicative of membrane and cytoplasmic damage. [32] It indicates that the cytoplasmic membranes, at this critical stage of meiotic prophase, are unstable and it is possible that oxidative metabolism in the Krebs cycle may be of major importance in the events leading to meiosis. Lysosomal activation and secondary lysosome formation has been found to be prominent in the injured cells.

Early round spermatids also show susceptibility to heat which causes late nuclear vacuolation of early round spermatids. These differences may be related to the difference in the temperature of heating. The delayed response suggests that metabolic changes in either the spermatids themselves or in the supporting Sertoli cells may be responsible for the nuclear abnormalities.

The histochemical staining of primary spermatocytes and round spermatids suggests the primary germ-cell stage undergoing apoptosis. Sperm and elongated spermatids have also been observed to stain for apoptosis in these experiments. Their absence from the seminiferous tubules, late in the course of experimental cryptorchidism may simply represent sloughing of the luminal portion of the germinal epithelium as the earlier stages undergo apoptosis.

It has been reported that the morphogenetic factor involved in development of the normal shape of the head shape of spermatozoa is the degree of chromatin packing during the process of spermiogenesis. Head abnormalities detected in epididymal sperm imply damage to the nuclei of late elongated spermatids. In addition, there is a possibility that oxidative stress leads to excessive generation of ROS in the apoptotic cells and defective spermatozoa. This in turn causes alterations in sperm parameters after 30 days of heat treatment.

The Leydig cells in all groups appeared to have been affected by the heat-treatment in the current study. Short photoperiod exposure (which reflects short days of the year) may result in hypofunction of the Leydig cells in testis of rats with possible consequent decrease in testosterone secretion and reproductive regression. Detailed metabolic and enzymatic studies of individual cell types in the testis are now necessary to determine more closely the changes produced by heat and other injurious agents. Experiments on bilateral cryptorchid mouse models have revealed that Leydig cell hypertrophy and hyperplasia is accompanied by an increase in smooth endoplasmic reticulum and mitochondria. [33] In contrast, it has been reported that steroidogenic functions of the somatic cells (Leydig and Sertoli cells) appear to be normal when exposed to the core body temperature. [34]

Bcl-2 and Bax proteins have also been implicated as potential modulators of germ cell apoptosis. In rats and monkeys, heat stress induces translocation of the proapoptotic protein Bax from the cytoplasm to the mitochondria of spermatozoa where it helps to release cytochrome *c*. [35] The integrity of mitochondria, which is established by the presence of cytochrome c in the space bounded by inner membrane, is lost by high ROS production. Release of series of such proteins from mitochondrial inner space is likely to accelerate the process of apoptosis, possibly leading to DNA damage. During heat stress, the proteins caspase-9 and 3 (hallmarks of apoptosis) become active, and their pharmacological inhibition prevents death of germ cells. It has also been proposed that apoptosis in the germ cells is related to the Fas signaling system that is activated by exogenous toxicants. [36]

Few researchers have found that stress interferes with reproduction and the functioning of the brain-pituitary-gonad (BPg) axis and cortisol has frequently been indicated as a major factor mediating the suppressive effect of stress on reproduction. [37] It has also been suggested that cortisol acts directly on Sertoli cells and/or on germ cells and induces retardation of testicular development as a result of heat stress. Chronically elevated glucocorticoids are suggested to have adverse effects on reproductive system. [38] It has been found that glucocorticoids affect both steroidogenesis, spermatogenesis and cause spermatogenic arrest at a certain stages of development of germ cells, in consistent with the results of the current study.

The synergistic action of FSH and testosterone has been found to be necessary to normalize the quantitative aspects of spermatogenesis. [39] As the Sertoli cell contains receptors for both FSH and testosterone, it is likely that these hormones exert their influence on germ cells by modulating functions of Sertoli cells. It has been observed that both LH and testosterone are responsible for normal spermatogenesis in male rats. [40] However, it has been suggested that of the two hormones only testosterone, and not FSH, is necessary. [41] Testosterone has its major intratesticular effect on the conversion of round spermatids to elongating spermatids in rats, whereas the major role of FSH is earlier in the spermatogenic process.

In normal testicular function, both Sertoli cells and Leydig cells are central to the regulation of fertility and reproductive health. It is well known that the Sertoli cells are susceptible to heat induced testicular damage. Sertoli cells, which are metabolically active, producing protein which aids in specific steps of germ cell maturation and steroids. In the current investigation, damage to Sertoli cells was evident in the heat-treated animals. The damage was characterized by cytoplasmic vacuolization and mitochondrial damage. After taking into account the related references, it can be inferred that the ultrastructural defects in spermatocytes and spermatids, particularly in those that interfere with the spermiation process, could be because of disturbances that affect the protein synthesis machinery essential for germ cell differentiation. Persistent damage to the Sertoli cells may have resulted in faulty spermatid differentiation, which ultimately led to azoospermia. Treatment-induced vacuolation of the Sertoli cells resulted in changes or decreases in seminiferous tubule fluid secretion, which further resulted in apical sloughing and germ cell death. These changes led to cytoplasmic vacuolization and nuclear pyknosis, without loss of germ cells or Sertoli cells affecting the process of spermatogenesis.

CONCLUSION

It is concluded from this study that daily exposure to heat for a period of 30 days results in apoptotic changes in the seminiferous tubules of the testis, indicated by sparse cytoplasmic organelles and vacuolation in Sertoli cells, and nuclear pyknosis in spermatocytes and spermatids. In particular, nuclear decondensation, acrosome formation and mitochondria are affected, which in turn result in defective spermatozoon production in the testes, reflected in abnormalities and loss of motility and sperm number. The treatment with mica nanoparticles successfully ameliorates the degenerative changes in seminiferous tubules and restores normalcy in structure and functions of the tubules. Thus nanomica is effective in preventing or reversing the infertility induced by heat stress.

ACKNOWLEDGEMENT

I greatly acknowledge the help rendered by the Lab Staff of R. J. College, Ghatkopar, and Mumbai, India. The full cooperation of Dr. Usha Mukundan, Principal, R. J. College, Ghatkopar, and Mumbai, India is worth mentioning. My heartfelt thanks to Dr Serena Dsouza, NRRI, Pune, India for helping me in reading the slides. Timely help and guidance of staff of Electron Microscopic Department of Jaslok Hospital, Mumbai, and India is highly appreciated.

REFERENCES

1. Hess RA. Spermatogenesis, Overview: Encyclopedia of Reproduction. Academic Press, 1999; **4:** 539-45.
2. Creasy DM. Use of Spermatogenic Staging. Toxico Patho, 1997**; 25(2):** 119-31.
3. Hess RA. Quantitative and qualitative characteristics of the stages and transitions in the cycle of the rat seminiferous epithelium: light microscopic observations of perfusion-fixed and plastic-embedded testes'. Bio Repro, 1990; **43:** 525-42.
4. Maller O, Martinson H, Schedin P. Extracellular matrix composition reveals complex and dynamic stromal-epithelial interactions in the mammary gland. J Mamm Gland Bio Neoplasia, 2010; **15(3):** 301-18.
5. Pop OT, Cotoi CG, Pleşea IE, Gherghiceanu MG, Enache SD et *al*. Histological and ultrastructural analysis of the seminiferous tubule wall in ageing testis. Rom J Morphol Embryol, 2011; **52(1):** 241–48.
6. Karp G. Cell and molecular biology: concepts and experiments. John Wiley & Sons, Inc.: 2010, 6th edition.

7. Alberts B, Johnson A, Lewis J. Molecular biology of the cell. New York: Garland Science: 2002, 4th edition.
8. Johnson L, Staub C, Neaves WB, Yanagimachi R. Live human germ cells in the context of their spermatogenic stages. Hum Reprod, 2001; **16(8):** 1575–82.
9. Yuan W, Leisner TM, McFadden AW, Clark S, Hiller S et *al*. CIB1 Is essential for mouse spermatogenesis. Mol Cell Biol, 2006; 26**(22):** 8507–14.
10. Ahuja MS. Gametogenesis and microscopic structure of gametes and early embryo. Manual of Assisted Reproductive Technologies and Clinical Embryology. JP Medical Ltd: 2011; Chapter **6:** pp 58.
11. Morgan JA, Cheepala SB, Wang Y, Neale G, Adachi M *et al*. Deregulated hepatic metabolism exacerbates impaired testosterone production in Mrp4-deficient mice J. Biol. Chem, 2012; **287:** 14456-66.
12. Gartner LP and Hiatt JL. Concise histology. Elsevier Health Sciences: 2010.
13. Lue Y, Hikim AP, Swerdloff RS, Im P, Taing KS *et al*. Single Exposure to Heat Induces Stage-Specific Germ Cell Apoptosis in Rats: Role of Intratesticular Testosterone on Stage Specificity. Endocrinol, 1999; 140**(2):** 852-58.
14. Hair WM, Wu FCW. Male contraception: prospects for the new millennium. Asian J Androl, 2000; **2:** 3-12.
15. Setchell B. The effects of heat on the testes of mammals. Anim Reprod, 2006; **3:** 81.
16. Jégou B. Spermatids are regulators of Sertoli cell function. Ann N Y Acad Sci, 1991; **637:** 340-53.
17. Galil KA and Setchell BP. Effects of local heating of the testis on testicular blood flow and testosterone secretion in the rat. Int J Androl, 1988; **11:** 73.
18. Yamamoto CM, Hikim APS, Huynh PN, Shapiro B, Lue Y *et al*. Redistribution of Bax is an early step in an apoptotic pathway leading to germ cell death in rats, triggered by mild testicular hyperthermia. Bio Reprod, 2000; **63(6):** 1683-90.
19. Rockett JC, Mapp FL, Garges JB, Luft JC, Mori C. Effects of hyperthermia on spermatogenesis, apoptosis, gene expression and fertility in adult male mice. Bio Reprod, 2001; **65(1):** 1229-239.
20. Blackshaw AW, Hamilton D, Massey PF. Effect of scrotal heating on testicular enzymes and spermatogenesis in the rat. Aust. J. Bio Sci, 1973; **26:** 1395-407.
21. Sailer BL, Sarkar LJ, Biordahi JA, Jost LK, Evenson DP. Effects of heat stress on mouse testicular cells and sperm chromatin structure. J Androl, 1997; **18(3):** 294-301.

22. Damber JE, Bergh A, Janson PO. Leydig cell function and morphology in the rat testis after exposure to heat. Andrologia, 1980; 12**(1):**12-19.
23. Meena MK, Khushwah HK, Rajagopala M, Ravishankar B. An experimental evaluation on nephroprotective activity of nagaradi kashaya. AYU Int Res J Ayurveda, 2009; **30(1):** 55-61.
24. CCRAS: Guidelines for toxicity / safety profile evaluation Of Bhasma/raskalpas: Standard Operating Procedure (SOP) for Administration of Bhasma/Rasakalpas with Honey as Vehicle. Available from: ccras.nic.in/pdf/Guidelinesfortoxicitybhasma.doc
25. Johnson L, Staub C, Neaves WB, Yanagimachi R. Live human germ cells in the context of their spermatogenic stages. Hum Reprod, 2012; **16(8):** 1575–82.
26. Kanter M, Aktas C, Erboga M. Heat stress decreases testicular germ cell proliferation and increases apoptosis in short term: an immunohistochemical and ultrastructural study**.** Toxico Ind Health, 2011; **29(2):** 99-113.
27. Kumar V, Abbas AK, Aster JC. Robbins Basic Pathology. Elsevier: 2012; 9th edition.
28. Creasy DM. Use of Spermatogenic Staging. Toxico Patho, 1997; **25(2):** 119-31.
29. Wang C, Cui Y, Wang X, Jia Y, Hikim AS. Transient scrotal hyperthermia and levonorgestrel enhance testosterone-induced spermatogenesis suppression in men through increased germ cell apoptosis. J Clin Endo Metabol, 2007; **92(8):** 3292-304.
30. Shokri S, Hemadi M, Aitken RJ. Transmission Electron Microscopy for the Quantitative Analysis of Testis Ultra Structure, The Transmission Electron Microscope. Dr. Khan Maaz (Ed.). InTech: 2012; Chap 7. Available from: http://www.intechopen.com/books/the-transmission-electron- microscope/transmission-electron-microscopy-for-the-quantitative-analysis-of-testis-ultra-structure
31. Franco R, Sanchez-Olea R, Reyes-Reyes E, Panayiotidis M. Environmental toxicity, oxidative stress and apoptosis: Menage a Trois Gent Toxico Envn Mutagen, 2009; **674(1-2):** 3-22.
32. Blackshaw AW, Hamilton D, Massey PF. Effect of scrotal heating on testicular enzymes and spermatogenesis in the rat. Aust J Bio Sci, 1973; **26:** 1395-407.
33. Absalan F, Movahedin M, Mowla SJ. Assessment of testis histological changes and sperm parameters in experimentally–induced unilateral and bilateral cryptorchid mouse model. Iran J Rep Med, 2008; **6(3):** 143-48.
34. Hall DM, Oberley TD, Moseley PM, Buettner GR, Oberley LW. Caloric restriction improves thermotolerance and reduces hyperthermia-induced cellular damage in old rats. Faseb J, 2000; **14(1):** 78-86.

35. Reyes JG, Farias JG, Henríquez-Olavarrieta S, Madrid E, Parraga M *et al*. The hypoxic testicle: Physiology and Pathophysiology. Oxid Med Cell Longev. 2012 (2012), **Article ID 929285:** 15.
36. Lee N and Cheng CY. Ectoplasmic specialization, a testis-specific cell–cell actin-based adherens junction type: is this a potential target for male contraceptive development? Hum Reprod, *2004*; **10(4):** 349-69.
37. Consten D, Keuning ED, Bogerd J, Zandbergen MA, Lambert JGD *et al.* Sex steroids and their Involvement in the cortisol-induced inhibition of pubertal development in male common carp, *Cyprinus carpio* L. Bio Repro, 2002; **67(2):** 465-72.
38. Wahbah NS, Abd El- Fattah EA, Ahmed FE, Hassan EZ. Histological study of the effect of exogenous glucocorticoids on the testis of prepubertal albino rat. Egypt J Histol, 2010; **33(2):** 353-64.
39. Wagner A and Claus R. Involvement of glucocorticoids in testicular involution after active immunization of boars against GnRH. Repro, *2004*; **127**: 275-83.
40. Griffin DK, Ellis PJ, Dunmore B, Bauer J, Abel MH *et al*. Transcriptional profiling of Luteinizing Hormone receptor-deficient mice before and after testosterone treatment provides insight into the hormonal control of postnatal testicular development and Leydig Cell differentiation. Bio Reprod; 2010; **82(6):** 1139-150.
41. Niu K, Chang C, Lin M, Huang K. A hyperbaric oxygen therapy approach to heat stroke with multiple organ dysfunctions. Chin J Physio, 2009; **52(3):** 169-72.